Supplementary Figure 1 submitted by the authors (Li Wang, Pengzhan Ying, Yuan Deng, Hong Zhou, Zhengliang Du, Jiaolin Cui)

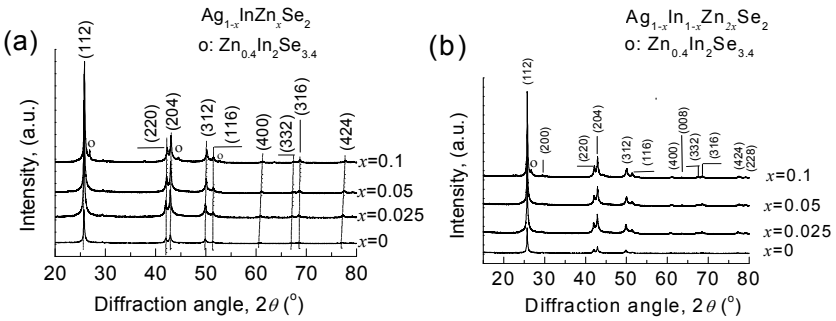

Supplementary Figure 1 X–ray diffraction patterns of the powders (a) $Ag_{1-x}InZn_xSe_2$, and (b) $Ag_{1-x}In_{1-x}Zn_{2x}Se_2$.

Supplementary Figure 2 submitted by the authors (Li Wang, Pengzhan Ying, Yuan Deng, Hong Zhou, Zhengliang Du, Jiaolin Cui)

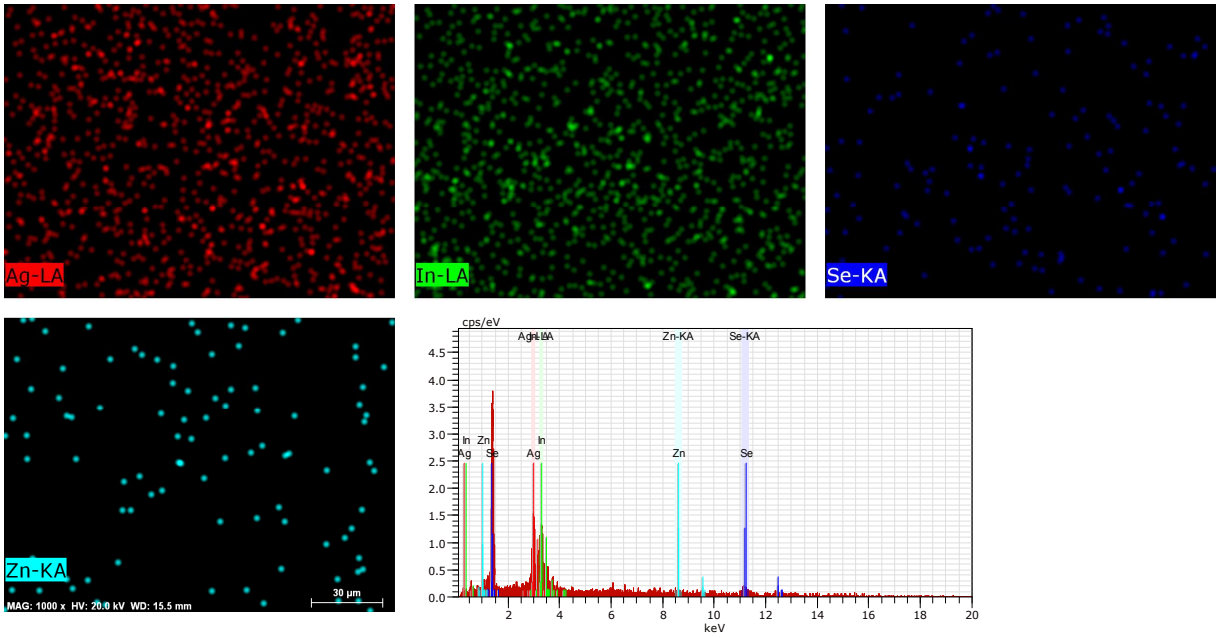

Supplementary Figure 2 A mapping of EPMA and energy dispersive x–ray spectra of $Ag_{1-x}In_{1-x}Zn_{2x}Se_2$ (x=0.1).

Supplementary Figure 3 submitted by the authors (Li Wang, Pengzhan Ying, Yuan Deng, Hong Zhou, Zhengliang Du, Jiaolin Cui)

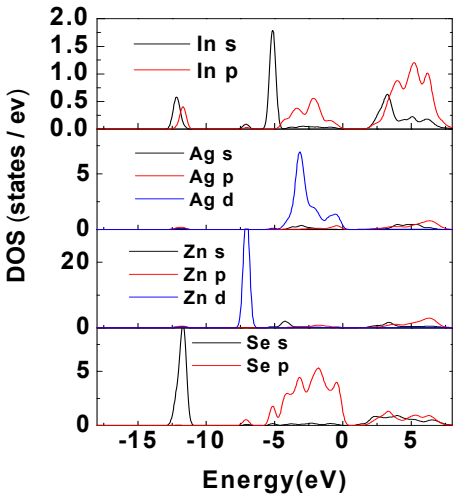

Supplementary Figure 3 Partial density of States (DOS) of different elements in Zn substituted $AgInSe_2$.

Supplementary Figure 4 submitted by the authors (Li Wang, Pengzhan Ying, Yuan Deng, Hong Zhou, Zhengliang Du, Jiaolin Cui)

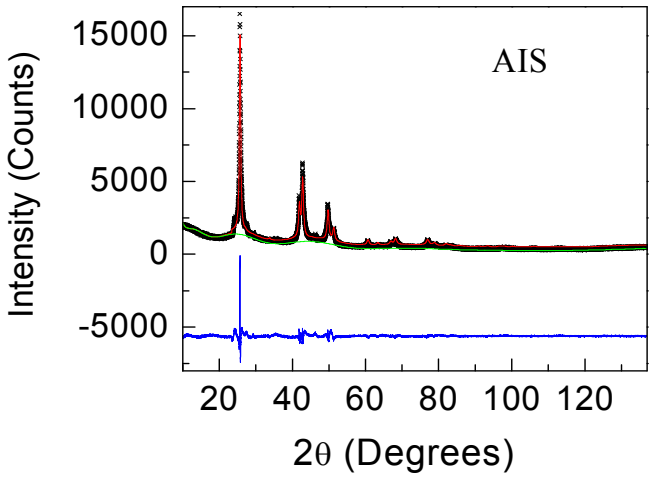

Supplementary Figure 4 Rietveld refinement using X-ray diffraction (w_{Rp}=0.0732 and Rp=0.0556) data for $AgInSe_2$. The goodness of fit $\chi 2$=1.612. Observed (×××) and calculated (solid line) X-ray powder diffraction patterns are shown.

Supplementary Figure 5 submitted by the authors (Li Wang, Pengzhan Ying, Yuan Deng, Hong Zhou, Zhengliang Du, Jiaolin Cui)

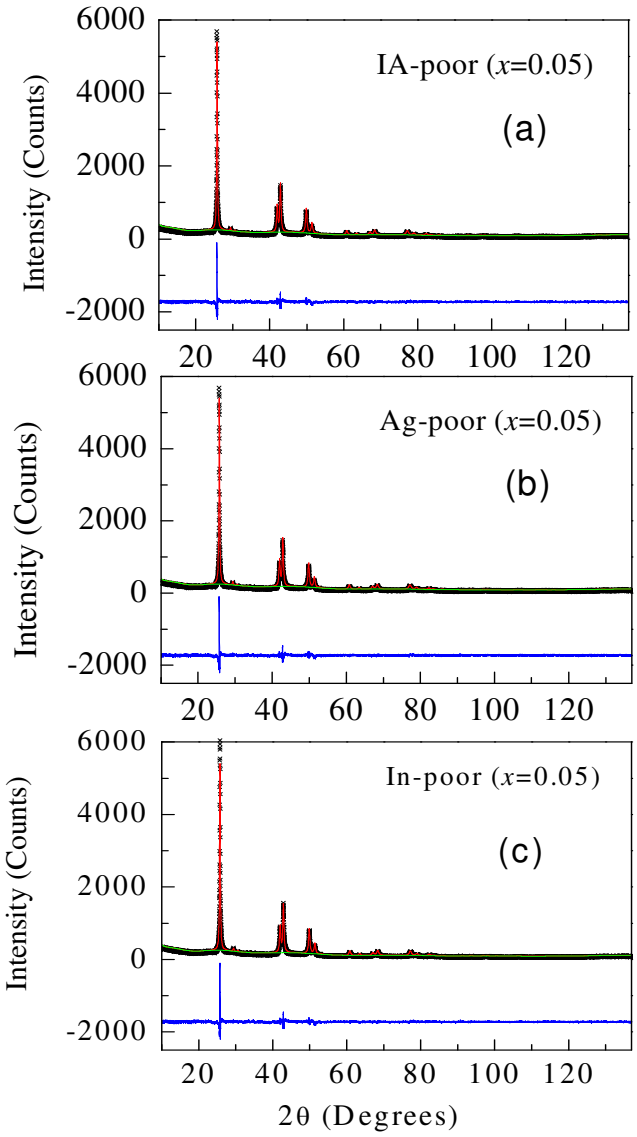

Supplementary Figure 5 Rietveld refinement using X-ray diffraction data for (a) IA–poor, (b) Ag–poor and (c) In–poor with x = 0.05. Observed (×××) and calculated (solid line) X-ray powder diffraction patterns are shown.

Supplementary Figure 6 submitted by the authors (Li Wang, Pengzhan Ying, Yuan Deng, Hong Zhou, Zhengliang Du, Jiaolin Cui)

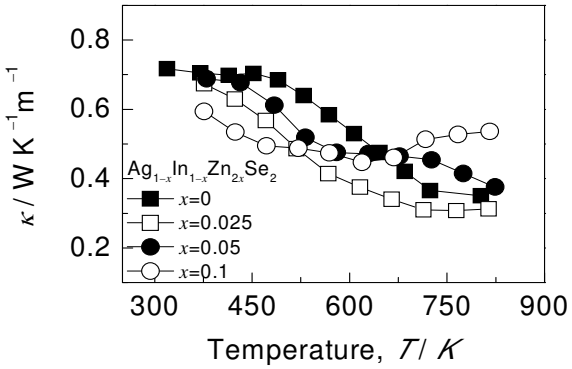

Supplementary Figure 6 Thermal conductivities (κ) of $Ag_{1-x}In_{1-x}Zn_{2x}Se_2$ as a function of the temperature.

Supplementary Figure 7 submitted by the authors (Li Wang, Pengzhan Ying, Yuan Deng, Hong Zhou, Zhengliang Du, Jiaolin Cui)

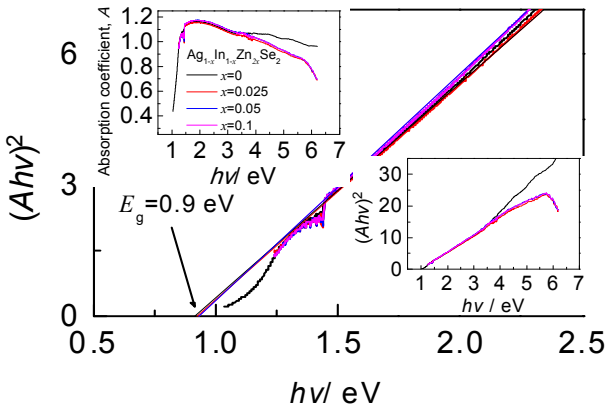

Supplementary Figure 7. Experimentally determined bandgap E_g of $Ag_{1-x}In_{1-x}Zn_{2x}Se_2$. An upper left insert is the absorption coefficient spectra A ($h\nu$), A is the absorption coefficient, $h\nu$ is the photon energy, and low right insert is the full relations of $(Ah\nu)^2 = (h\nu - E_g)$.

Supplementary Figure 8 submitted by the authors (Li Wang, Pengzhan Ying, Yuan Deng, Hong Zhou, Zhengliang Du, Jiaolin Cui)

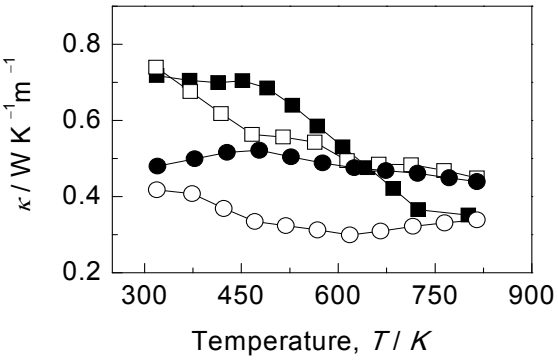

Supplementary Figure 8 Thermal conductivities (κ) of $Ag_{1-x}InZn_xSe_2$ as a function of the temperature.

Supplementary Figure 9 submitted by the authors (Li Wang, Pengzhan Ying, Yuan Deng, Hong Zhou, Zhengliang Du, Jiaolin Cui)

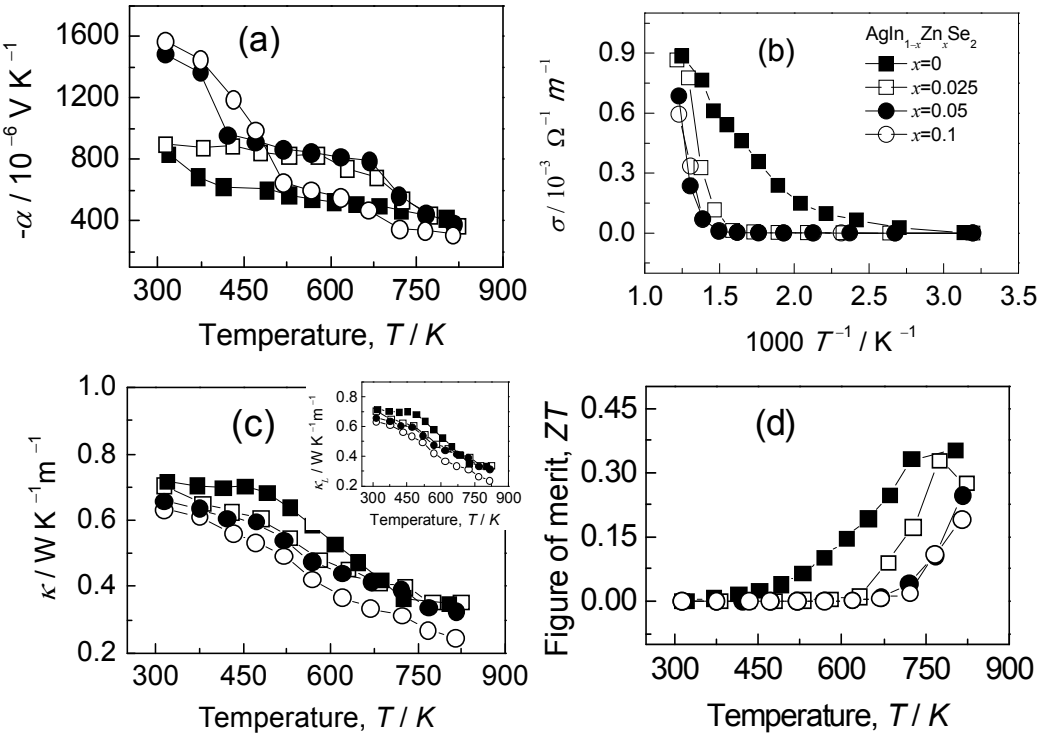

Supplementary Figure 9 Thermoelectric properties of $AgIn_{1-x}Zn_xSe_2$, (a) Seebeck coefficients (α), (b) electrical conductivities (σ), (c) Thermal conductivities (κ), an insert is the relation of κ_L–T, (d) ZT values.

Supplementary Figure 10 submitted by the authors (Li Wang, Pengzhan Ying, Yuan Deng, Hong Zhou, Zhengliang Du, Jiaolin Cui)

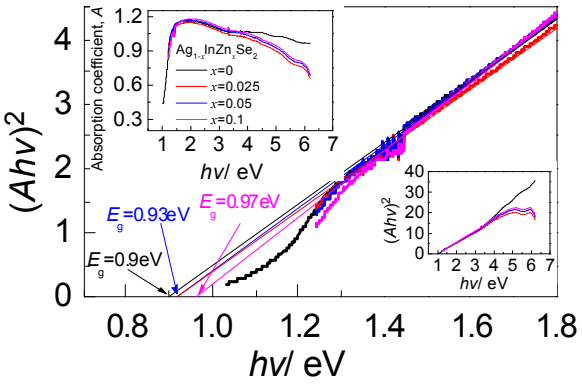

Supplementary Figure 10 Experimentally determined bandgap E_g of $Ag_{1-x}InZn_xSe_2$. An upper left insert is the absorption coefficient spectra A $(h\nu)$, and low right insert is the full relations of $(Ah\nu)^2 = (h\nu - E_g)$.

Supplementary Figure 11 submitted by the authors (Li Wang, Pengzhan Ying, Yuan Deng, Hong Zhou, Zhengliang Du, Jiaolin Cui)

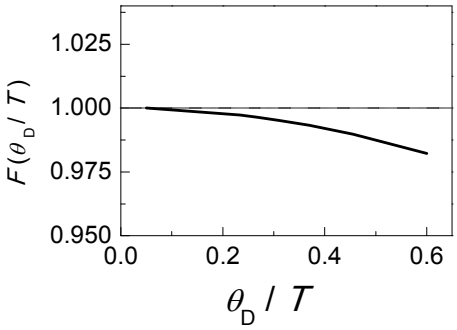

Supplementary Figure 11 Debye function $F(\theta_D/T)$ as a function of θ_D/T used in the estimation of the heat capacities (C_p) of $AgInSe_2$ based semiconductors.

Supplementary Table 1 submitted by the authors (Li Wang, Pengzhan Ying, Yuan Deng, Hong Zhou, Zhengliang Du, Jiaolin Cui)

Supplementary Table 1 The chemical compositions (relative molars) identified using EPMA for $Ag_{1-x}InZn_xSe_2$, $Ag_{1-x}In_{1-x}Zn_{2x}Se_2$ (x=0, 0.1) (taken from a mapping)

Sample	x	Ag	In	Zn	Se
AIS		1.02	1.04		1.94
IA–AIS	0.10	0.91	0.94	0.19	1.96
Ag–AIS	0.10	0.92	1.02	0.09	1.97

Supplementary Table 2 submitted by the authors (Li Wang, Pengzhan Ying, Yuan Deng, Hong Zhou, Zhengliang Du, Jiaolin Cui)

Supplementary Table 2 Structural Parameters for $AgInSe_2$ Obtained by Rietveld Refinements

atom	Wyc	*x*	*y*	*z*	SOF	100Uiso [Å^2]
Ag	4*a*	0	0	0	0. 9522 (2)	2.2020 (5)
In	4*b*	0	0	0.5	0.9956 (3)	2.3820 (5)
Se	8*d*	0.2341(3)	0.25	0.125	0.9720 (4)	1.5840 (4)

Supplementary Table 3 Structural parameters and refinement details for IA–poor compounds ($Ag_{1-x}In_{1-x}Zn_{2x}Se_2$) obtained by Rietveld refinements

Parameters	x = 0.025		x = 0.05	
	Model B	Model C	Model B	Model C
		Cation 4*a*		
SOF(Ag)	0.9832(5)	0.9750(4)	0.9588(4)	0.9500(2)
SOF(Zn)	0.0277(4)	0.0244(5)	0.0316(8)	0.0593 (4)
SOF(In)	0	0.0081(3)	0	0.0002(2)
100Uiso [Å^2]	2.0040(10)	1.9880(7)	2.1130(10)	1.8770(7)
		Cation 4*b*		
SOF(In)	0.9750(3)	0.9814(5)	0.9500(2)	0.9498(4)
SOF(Zn)	0.0233(7)	0.0256(4)	0.0684(3)	0.0407(2)
SOF(Ag)	0.0008(1)	0	0.0088(4)	0
100Uiso [Å^2]	2.2380(9)	2.1860(7)	2.2740(7)	2.2370(6)
		Anion 8*d*		
SOF(Se)	0.9729(2)	0.9814(5)	0.9474(4)	0.9825(1)
100Uiso [Å^2]	1.6270(9)	1.5740(9)	1.562(3)	1.588(3)
x_{Se}	0.2398(3)	0.2385(3)	0.2391(2)	0.2393(2)
		Reliability factors		
χ^2	1.8210	1.8250	1.5870	1.5790
wR_p	0.0975	0.0976	0.0886	0.0884
R_p	0.0778	0.0778	0.0705	0.0703

Supplementary Table 4 Structural parameters and refinement details for In–poor and Ag–poor compounds (x=0.05) obtained by Rietveld refinements

Parameters	In–poor		Ag–poor	
	Model B	Model C	Model B	Model C
		Cation 4*a*		
SOF(Ag)	0.9945(7)	1.0000(4)	0.9422(5)	0.9500(2)
SOF(Zn)	0.0002(6)	0.0009(3)	0.0578(6)	0.0566(7)
SOF(In)	0	0.0058(2)	0	0.0003(4)
100Uiso [Å^2]	1.9450(6)	1.9700(5)	2.1070(4)	2.0590(6)
		Cation 4*b*		
SOF(In)	0.9500(4)	0.9403(6)	1.0000	0.9997(1)
SOF(Zn)	0.0498(6)	0.0442(8)	0	–0.0066(3)
SOF(Ag)	0.0005(2)	0	0	0
100Uiso [Å^2]	2.2550(6)	2.3730(6)	2.3260(8)	2.3670(6)
		Anion 8*d*		
SOF(Se)	0.9670(5)	0.9941(3)	0.9645(3)	0.9843(3)
100Uiso [Å^2]	1.3680(3)	1.3730(6)	1.2960(8)	1.5760(7)
x_{Se}	0.2438(3)	0.2465(2)	0.2380(3)	0.2394(2)
		Reliability factors		
χ^2	1.7080	1.6870	1.6870	1.6840
wR_p	0.0976	0.0970	0.0929	0.0928
R_p	0.0761	0.0760	0.0736	0.0736